J. Fluid Mech. (2003), *vol.* 476, *pp.* 159–177.
DOI: 10.1017/S0022112002003026 Printed in the United Kingdom

On steady Stokes flow in a trihedral rectangular corner

By A. M. GOMILKO, V. S. MALYUGA AND V. V. MELESHKO

Institute of Hydromechanics, National Academy of Sciences, 03680 Kiev, Ukraine

(Received 15 January 2002 and in revised form 23 August 2002)

Motivated by the recent paper of Hills & Moffatt (2000), we investigate the Stokes flow in a trihedral corner formed by three mutually orthogonal planes, induced by a non-zero velocity distribution over one of the walls of the corner. It is shown that the local behaviour of the velocity field near the edges of the corner, where a discontinuity of the boundary velocity is assumed, coincides with the Goodier–Taylor solution for a two-dimensional wedge. Analysis of the streamline patterns confirms the existence of eddies near the stationary edge in the flow, induced either by uniform translation of one of the walls of the corner in the direction perpendicular to its bisectrix or by uniform rotation of a side about the vertex of the corner. These flows are shown to be quasi-two-dimensional. If the wall rotates about a centre displaced from the vertex, the induced flow is essentially three-dimensional. In the antisymmetric velocity field, a stagnation line appears composed of stagnation points of different types. Otherwise the three-dimensionality manifests itself in a non-closed spiral shape of the streamlines.

1. Introduction

The study of laminar motion of a viscous incompressible fluid in a container bounded by a surface with singular points is an interesting problem in fluid mechanics that involves considerable mathematical difficulties (Shankar & Deshpande 2000). The problem may be complicated even more by the presence of a discontinuity in the velocity at the edge at the boundary. Within the limits of the linear approximation of the problem, this difficulty may be readily overcome provided the local behaviour of the flow field near the points of discontinuity is known. Indeed, since the superposition principle is valid, the solution may be presented as a superposition of the known solution responsible for the discontinuity of the prescribed velocity and some new solution satisfying continuous boundary conditions. One example is the Stokes problem in a driven cubic cavity where the motion of the lid generates the fluid motion. Although the geometry of the problem and the governing equations appear simple, the asymptotic behaviour of the flow near the corners is still unresolved.

Stokes flow in a two-dimensional corner has been studied extensively by many authors. The flow induced by the steady motion of one of the walls of the corner parallel to itself is described by the well-known solution by Goodier (1934) and Taylor (1962). The flow in a corner with fixed sides, induced by an arbitrary disturbance far away from the vertex, was studied by Dean & Montagnon (1949) and Moffatt (1964). It was shown that, provided that the corner angle is less than some critical value, an

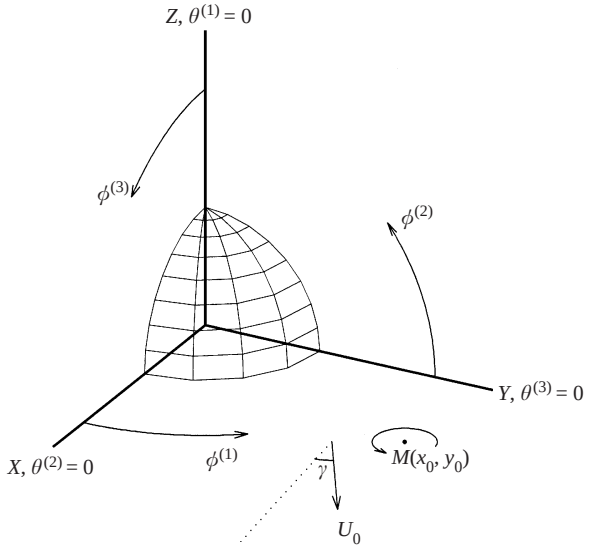

FIGURE 1. Geometry of the problem. Three spherical coordinate systems $(r, \theta^{(i)}, \phi^{(i)})$, $i = 1, 2, 3$, with a common origin at the vertex of the corner. The three axes $\theta^{(i)} = 0$ coincide with the three edges of the corner. The coordinate curves of the system $(r, \theta^{(1)}, \phi^{(1)})$ are shown on a sphere.

infinite sequence of eddies of decreasing size and strength would be generated. The Poiseuille flow in a dihedral corner was studied by Moffatt & Duffy (1980).

It is natural to expect that in a trihedral corner the three-dimensional flow field behaves near the edges in accordance with the aforementioned two-dimensional solutions. Hills & Moffatt (2000) analysed the asymptotic behaviour of the flow near the edge formed by two fixed triangular fins placed in a rotating cone and concluded that there exists a sequence of eddies. The streamlines of the eddies lie on concentric spheres with the centre at the cone's vertex. This result was extended to the trihedral corner treated as a cone of angle $\pi/2$ with the fins. A similar conclusion was reached by Shankar (2000) who studied the Stokes problem in a trihedral corner with a non-zero boundary velocity assigned within some ring at a corner's wall. He established the existence of corner eddies in the antisymmetric flow and found non-closed spirally shaped streamlines. This complicated behaviour was caused by the three-dimensional nature of the flow.

This paper concerns the Stokes flow in the trihedral corner formed by three mutually orthogonal planes. The flow is induced by a non-zero tangential velocity prescribed at one of the walls of the corner. The prescribed velocity is assumed to take non-zero values at the edges. The technique developed in the paper is based on the method of superposition, in the framework of which the velocity field is presented as a sum of three vector fields. Each of them, being a solution of the Stokes equations, is constructed in one of three spherical coordinate systems $(r, \theta^{(i)}, \phi^{(i)})$, $i = 1, 2, 3$, with a common origin at the vertex of the corner. These systems are introduced in such a way that any wall of the corner lies in the equatorial plane of the corresponding coordinate system (figure 1). It is well known that the Stokes equations admit a representation of the velocity as a power of the radial spherical coordinate $\boldsymbol{U} = Ar^n \boldsymbol{u}$, where $\boldsymbol{u}$ depends only on the physical coordinates, and A is some dimensional velocity. We consider two typical cases, namely $n = 0$ and $n = 1$, corresponding to the simplest and practically realizable examples of uniform translation and uniform rotation of

the wall around the origin. Both flows are shown to be quasi-two-dimensional, and the differential equations for the streamlines are integrable, and its integral expresses the radial coordinate $r$of a fluid particle via its geographical coordinates. The flow becomes essentially three-dimensional as the centre of the wall rotation is displaced from the vertex. Depending upon the centre's position, this results either in the appearance of a stagnation line composed of stagnation points of different types or in the appearance of non-closed spirally shaped streamlines. The conclusion by Hills & Moffatt (2000) concerning the sequence of eddies is confirmed by the analysis of the streamline patterns. It is shown that the principal term of the velocity field near the edge, where one wall scrapes along the other, coincides with the Goodier–Taylor solution for a two-dimensional wedge.

To conclude the Introduction it is necessary to determine for what range of values of r the Stokes approximation is valid in the corner. For the solutions of the form $\boldsymbol{U} = Ar^n \boldsymbol{u}$, the analysis is similar to that of Moffatt (1964) for a two-dimensional corner. The Reynolds number

$$Re = \frac{Ar^{n+1}}{\nu} \tag{1.1}$$

is based on distance from the vertex. Here ν is the kinematic viscosity of a liquid. Hence, the inertial forces in both cases ($n = 0$ and $n = 1$) are negligible in the neighbourhood of the vertex.

Near the boundary, the applicability of the Stokes approximation is not so evident. However, exploiting the fact established later in the paper that in the vicinity of the edge, where one wall is scraped by the other, say $\theta^{(2)} = 0$, the velocity field behaves in accordance with the Goodier–Taylor solution, one can estimate the orders of the inertial and viscous forces near the edge:

$$\boldsymbol{U} \cdot \nabla \boldsymbol{U} = O\left(\frac{A^2 r^{2n-1}}{\sin\theta^{(2)}}\right), \quad \nu \nabla^2 \boldsymbol{U} = O\left(\frac{\nu A r^{n-2}}{\sin^2\theta^{(2)}}\right), \quad \theta^{(2)} \to 0. \tag{1.2}$$

The ratio of these terms provides the local Reynolds number near the edge

$$Re = \frac{Ar^n \rho}{\nu}, \tag{1.3}$$

where $\rho = r \sin\theta^{(2)}$ is distance from the edge. Hence, near the edges of the trihedral corner, the inertial forces are negligible at any distance from the vertex provided the distance from the edge is sufficiently small.

The paper is organized as follows: the formulation of the general problem is described in § 2. The analytical solution method is described in § 3 along with considerations of the correct reduction of the infinite system, and theoretical considerations of the local behaviour of the velocity field near the edges. Next, § 4 contains some numerical results concerning three typical cases of flows in the trihedral corner. The structure of the closed streamlines is revealed in detail based upon general considerations of the three-dimensional topology of the velocity field near a singular point. The complicated eddy structure is analysed related to the type of flow excitation. Finally, some conclusions related to the approach developed are given in § 5. Appendix A contains standard tranformations relating the unit and arbitrary vectors in different spherical coordinate systems with a common origin, and Appendix B contains the right-hand sides of the main infinite system of equations.

2. Statement of the problem

The flow to be considered occurs in a trihedral corner formed by three mutually orthogonal planes (figure 1). The region $x \geqslant 0$, $y \geqslant 0$, $z \geqslant 0$ between these planes is occupied by a homogeneous incompressible fluid of viscosity μ. In the low Reynolds number approximation, when the inertia forces are negligible in comparison to the viscous ones, the velocity vector $\boldsymbol{U}$ and the pressure P are governed by the linear system

$$\mu \nabla^2 \boldsymbol{U} = \nabla P, \tag{2.1a}$$

$$\nabla \cdot \boldsymbol{U} = 0, \tag{2.1b}$$

that represents the linearized vector equation of momentum (the Stokes approximation) and the continuity equation, respectively.

The creeping motion of the fluid is generated by motion of the bottom wall, $z = 0$, while the two sidewalls remain fixed. In what follows we consider three typical cases of motion of the bottom wall, namely a uniform translation with constant velocity of value U_0 in the direction of angle γ to the positive direction of the X-axis, a rotation with angular velocity Ω about the origin $O(0,0)$ and a rotation with angular velocity Ω about some point $M(x_0, y_0)$ displaced from the vertex – problems A, B and C, respectively, see figure 1.

The boundary conditions for the Cartesian components U_x, U_y, U_z of the velocity vector $\boldsymbol{U}$ at the immovable walls are

$$\left.\begin{aligned} &U_x = 0, \quad U_y = 0, \quad U_z = 0 \quad \text{at} \quad x = 0, \quad y > 0, \quad z > 0, \\ &U_x = 0, \quad U_y = 0, \quad U_z = 0 \quad \text{at} \quad y = 0, \quad x > 0, \quad z > 0. \end{aligned}\right\} \tag{2.2}$$

At the bottom wall $z = 0$

$$U_x = U_0 \cos\gamma, \quad U_y = U_0 \sin\gamma, \quad U_z = 0 \quad \text{at} \quad z = 0, \quad x \geqslant 0, \quad y \geqslant 0 \tag{2.3a}$$

for problem A, and

$$U_x = -\Omega\,(y - y_0), \quad U_y = \Omega\,(x - x_0), \quad U_z = 0 \quad \text{at} \quad z = 0, \quad x \geqslant 0, \quad y \geqslant 0 \tag{2.3b}$$

for problem B (with $x_0 = 0$, $y_0 = 0$) and for problem C in the general case.

It is evident that the boundary velocity in problem C is a sum of the boundary velocities in problems A and B when $U_0 \sin\gamma = -\Omega\, x_0$, $U_0 \cos\gamma = \Omega\, y_0$. In view of the linearity, a solution of problem C can be found as a sum of solutions of problems A and B.

It is important to point out that both of the conditions (2.3) provide non-zero values of the velocity components at the edges of the corner; in other words, there is a discontinuity of the applied velocity at the rims. One of the goals of our study is to find the correct behaviour of the continuous velocity field inside the corner under such a discontinuous applied velocity at the bottom wall.

2.1. *Spherical coordinates: a particular case*

In the case of problem B (the rotation about the origin O), the three-dimensional problem (2.1), (2.3b) can be reduced to a two-dimensional one. Indeed, by introducing a spherical coordinate system (r, θ, ϕ) with the origin at the vertex O, we may try to

look for the following form of the velocity and pressure:

$$\boldsymbol{U}(r,\,\theta,\,\phi) = r\,[u_r(\theta,\,\phi)\,\boldsymbol{e}_r + u_\theta(\theta,\,\phi)\,\boldsymbol{e}_\theta + u_\phi(\theta,\,\phi)\,\boldsymbol{e}_\phi], \quad P(r,\,\theta,\,\phi) = p(\theta,\,\phi). \tag{2.4}$$

Then, the continuity equation (2.1) written in spherical coordinates leads to

$$3\,u_r + \frac{1}{\sin\theta}\,\frac{\partial}{\partial\theta}\,(\sin\theta\,u_\theta) + \frac{1}{\sin\theta}\,\frac{\partial u_\phi}{\partial\phi} = 0, \tag{2.5}$$

while the first scalar equation in the system (2.1) provides the homogeneous scalar equation for the component u_r:

$$\mathrm{L}_\omega(u_r) + 6\,u_r = 0, \tag{2.6}$$

with the so-called Laplace–Beltrami operator on a sphere

$$\mathrm{L}_\omega = \frac{\partial^2}{\partial\theta^2} + \cot\theta\,\frac{\partial}{\partial\theta} + \frac{1}{\sin^2\theta}\,\frac{\partial^2}{\partial\phi^2}. \tag{2.7}$$

Next, the boundary condition (2.3*b*) written in terms of the spherical components of the velocity vector $\boldsymbol{U}$ provides $u_r = 0$ at $z = 0$. Therefore, we may put $u_r \equiv 0$, and the continuity equation (2.5) allows us to introduce the stream function $\Psi(\theta,\,\phi)$ such that

$$u_\theta = -\frac{1}{\sin\theta}\,\frac{\partial\Psi}{\partial\phi}, \quad u_\phi = \frac{\partial\Psi}{\partial\theta}. \tag{2.8}$$

Finally, both the second and third scalar equations in the Stokes vector equation (2.1) lead to the scalar equation

$$\mathrm{L}_\omega^2\,(\Psi) + 2\,\mathrm{L}_\omega\,(\Psi) = 0. \tag{2.9}$$

Thus, for the particular case $x_0 = 0$, $y_0 = 0$, the three-dimensional Stokes problem in the corner can be reduced to the two-dimensional problem on a sphere for the scalar function $\Psi(\theta,\,\phi)$ with appropriate boundary conditions resulting from (2.3*b*).

2.2. *Spherical coordinates: a general case*

The particular case of usage of the spherical coordinates in problem B suggests consideration of the general statement of the boundary problem (2.1)–(2.3) in such a coordinate system. In view of the method of solution which will be presented below, it is convenient to introduce three spherical coordinate systems $(r,\,\theta^{(i)},\,\phi^{(i)})$, $i = 1,\,2,\,3$, with a common origin O at the vertex of the corner. These systems are such that each of the corner walls lies in the equatorial plane of the corresponding coordinate system (figure 1). In each of these three spherical systems the corner occupies the first octant $0 \leqslant r < \infty$, $0 \leqslant \theta^{(i)} \leqslant \pi/2$, $0 \leqslant \phi^{(i)} \leqslant \pi/2$, $i = 1,\,2,\,3$.

The velocity vector $\boldsymbol{U} = U_r\,\boldsymbol{e}_r + U_{\theta^{(i)}}\,\boldsymbol{e}_{\theta^{(i)}} + U_{\phi^{(i)}}\,\boldsymbol{e}_{\phi^{(i)}}$ and the pressure $P(r,\,\theta^{(i)},\,\phi^{(i)})$ satisfy equations (2.1) written in the corresponding spherical coordinates. Note that the Laplace operator ∇^2 being applied to the vector $\boldsymbol{U}$ in the spherical coordinates provides another vector with components not equal to the scalar Laplacian of U_r, $U_{\theta^{(i)}}$, $U_{\phi^{(i)}}$ (see, for example, Batchelor 1967, Appendix 2 for the coordinate form of the governing equations). Relations between the components of the vector $\boldsymbol{U}$ in these coordinate systems are given by (A 4).

In further considerations we will use a more general form of the boundary conditions, namely

$$U_r = r^n f^{(i)}(\phi^{(i)}), \quad U_{\theta^{(i)}} = 0, \quad U_{\phi^{(i)}} = r^n g^{(i)}(\phi^{(i)}) \quad \text{at} \quad \theta^{(i)} = \tfrac{1}{2}\pi, \tag{2.10}$$

with arbitrary smooth functions $f^{(i)}$, $g^{(i)}$ $(i = 1, 2, 3)$ and $n = 0, 1, \ldots$. Such a form provides some compactness in analytical representations of the solution. For our problems we may put $n = 0$, $f^{(i)}(\phi^{(i)}) = 0$, $g^{(i)}(\phi^{(i)}) = 0$, when $i = 2$, 3, and $f^{(1)}(\phi^{(1)}) = U_0 \cos(\phi^{(1)} - \gamma)$, $g^{(1)}(\phi^{(1)}) = -U_0 \sin(\phi^{(1)} - \gamma)$ for problem A and $n = 1$, $f^{(1)}(\phi^{(1)}) = 0$, $g^{(1)}(\phi^{(1)}) = \Omega$ for problem B.

3. Method of solution

To solve the three-dimensional creeping flow problem we need, first, to construct the solution of the vector equations (2.1), and, secondly, to fulfil with that representation for the velocity vector all boundary conditions (2.10). Usually, the second step is far more difficult than the first one.

3.1. *Solution of the governing equations*

There are several approaches to constructing the representation of the velocity vector $\boldsymbol{U}$ for the Stokes equations (2.1). We will use a general solution in spherical coordinates in terms of three harmonic functions originally developed by Lamb (1932). A detailed description of Lamb's solution and its application to the solution of various creeping flow problems can be found in Happel & Brenner (1965).

If the harmonic pressure P is represented as a series of spherical harmonics

$$P = \mu \sum p_k, \tag{3.1}$$

then the velocity vector $\boldsymbol{U}$ is expressed in terms of three sequences of spherical harmonics

$$\boldsymbol{U} = \sum \left[\nabla \times (\boldsymbol{r}\chi_k) + \nabla \Phi_k + \frac{k+3}{2(k+1)(2k+3)} r^2 \nabla p_k - \frac{k}{(k+1)(2k+3)} \boldsymbol{r} p_k \right]. \tag{3.2}$$

Here $\nabla\times$ represents the curl of a vector, $\boldsymbol{r}$ is a radius vector of a point in the spherical coordinates (r, θ, ϕ), Φ_k, χ_k, p_k are solid spherical harmonics of order k of general form $r^k Z_k(\theta, \phi)$, with Z_k being a surface spherical harmonic, satisfying the equation

$$\mathrm{L}_\omega(Z_k) + k\,(k+1)\, Z_k = 0, \tag{3.3}$$

with the Laplace–Beltrami operator L_ω defined by (2.7). The first two terms of representation (3.2) are solutions of the homogeneous equations, corresponding to the governing equations (2.1), whereas the third and fourth terms represent a particular solution of the inhomogeneous equations.

In order to obtain sufficient functional arbitrariness to fulfil all boundary conditions (2.10) at the walls we represent the velocity and pressure fields as superpositions of three vector and scalar fields, respectively:

$$\boldsymbol{U} = r^n \sum_{i=1}^{3} \boldsymbol{u}^{(i)}(\theta^{(i)}, \phi^{(i)}), \quad P = \mu r^{n-1} \sum_{i=1}^{3} p^{(i)}(\theta^{(i)}, \phi^{(i)}). \tag{3.4}$$

Each pair of terms $r^n \boldsymbol{u}^{(i)}$, $\mu r^{n-1} p^{(i)}$ represents a solution of the Stokes equations in the

*i*th spherical coordinate system. They are determined from (3.1) and (3.2) as the terms with power dependence r^n and r^{n-1}, respectively. For $n \geqslant 1$ (the singular case $n = 0$ will be considered later) these functions have the following representation:

$$\left.\begin{aligned} p^{(i)} &= p^{(i)}_{n-1}, \quad u^{(i)}_r = (n+1)\,\Phi^{(i)}_{n+1} + \frac{n-1}{2\,(2n+1)}\,p^{(i)}_{n-1}, \\ u^{(i)}_{\theta^{(i)}} &= \frac{\partial \Phi^{(i)}_{n+1}}{\partial \theta^{(i)}} + \frac{1}{\sin\theta^{(i)}}\,\frac{\partial \chi^{(i)}_n}{\partial \phi^{(i)}} + \frac{n+2}{2n(2n+1)}\,\frac{\partial p^{(i)}_{n-1}}{\partial \theta^{(i)}}, \\ u^{(i)}_{\phi^{(i)}} &= \frac{1}{\sin\theta^{(i)}}\,\frac{\partial \Phi^{(i)}_{n+1}}{\partial \phi^{(i)}} - \frac{\partial \chi^{(i)}_n}{\partial \theta^{(i)}} + \frac{n+2}{2n(2n+1)}\,\frac{1}{\sin\theta^{(i)}}\,\frac{\partial p^{(i)}_{n-1}}{\partial \phi^{(i)}}. \end{aligned}\right\} \tag{3.5}$$

Here $\Phi^{(i)}_{n+1}$, $\chi^{(i)}_n$ $p^{(i)}_{n-1}$ denote three surface spherical harmonics in equation (3.3) for k equal to $n+1$, n, $n-1$, respectively. These functions can be chosen in the form of Fourier series on the complete trigonometric system on the interval $0 \leqslant \phi^{(i)} \leqslant \pi/2$

$$\left.\begin{aligned} \Phi^{(i)}_{n+1} &= \sum_{m=1}^{\infty} X^{(i,1)}_m\,\frac{P^{-2m}_{n+1}(\cos\theta^{(i)})}{P^{-2m}_1(0)}\,\sin 2m\phi^{(i)}, \\ \chi^{(i)}_n &= \frac{C^{(i)}}{n\,(n+1)}\,\frac{P_n(\cos\theta^{(i)})}{P^{-1}_n(0)} + \sum_{m=1}^{\infty} X^{(i,2)}_m\,\frac{P^{-2m}_n(\cos\theta^{(i)})}{P^{-2m}_1(0)}\,\cos 2m\phi^{(i)}, \\ p^{(i)}_{n-1} &= \sum_{m=1}^{\infty} X^{(i,3)}_m\,\frac{P^{-2m}_{n-1}(\cos\theta^{(i)})}{P^{-2m}_1(0)}\,\sin 2m\phi^{(i)}, \end{aligned}\right\} \tag{3.6}$$

with three sequences of as yet arbitrary coefficients $X^{(i,1)}_m$, $X^{(i,2)}_m$, $X^{(i,2)}_m$, and an arbitrary constant $C^{(i)}$. These sequences all depend on n but we omit this index without loss of clarity, restricting our further consideration to a fixed value of $n = 0$ or $n = 1$. Here $P_n(\zeta)$ is the Legendre polynomial and $P^{-2\mu}_\nu(\zeta)$ denotes the associated Legendre functions of the first kind, defined for $\nu = 0$ and $\nu = 1$ by

$$P^{-2\mu}_0(\zeta) = \frac{1}{\Gamma(2\mu+1)}\left(\frac{1-\zeta}{1+\zeta}\right)^{\mu}, \quad P^{-2\mu}_1(\zeta) = \frac{1}{\Gamma(2\mu+2)}\left(\frac{1-\zeta}{1+\zeta}\right)^{\mu}(2\mu+\zeta) \tag{3.7}$$

(where Γ is the gamma function), and by recurrence relations (Abramowitz & Stegun 1965, p. 334)

$$(\nu+1+2\mu)\,P^{-2\mu}_{\nu+1}(\zeta) = (2\nu+1)\,\zeta\,P^{-2\mu}_\nu(\zeta) + (2\mu-\nu)\,P^{-2\mu}_{\nu-1}(\zeta). \tag{3.8}$$

It follows from (3.5), (3.6) that the components of the vector $\boldsymbol{u}^{(i)}$ can be written in the form of Fourier series:

$$\left.\begin{aligned} u^{(i)}_r &= \sum_{m=1}^{\infty} q^{(i)}_m(\theta^{(i)})\,\sin 2m\phi^{(i)}, \quad u^{(i)}_{\theta^{(i)}} = \sum_{m=1}^{\infty} s^{(i)}_m(\theta^{(i)})\,\sin 2m\phi^{(i)}, \\ u^{(i)}_{\phi^{(i)}} &= C^{(i)}\,\frac{P^{-1}_n(\cos\theta^{(i)})}{P^{-1}_n(0)} + \sum_{m=1}^{\infty} t^{(i)}_m(\theta^{(i)})\,\cos 2m\phi^{(i)}, \quad i = 1,\,2,\,3\,, \end{aligned}\right\} \tag{3.9}$$

with the notation

$$q_m^{(i)} = (n+1)X_m^{(i,1)}\,\frac{P_{n+1}^{-2m}(\cos\theta^{(i)})}{P_1^{-2m}(0)} + \frac{n-1}{2(2n+1)}X_m^{(i,3)}\,\frac{P_{n-1}^{-2m}(\cos\theta^{(i)})}{P_1^{-2m}(0)}, \tag{3.10}$$

$$\left.\begin{aligned} s_m^{(i)} &= X_m^{(i,1)}\,\frac{P_{n+1}^{-2m\prime}(\cos\theta^{(i)})}{P_1^{-2m}(0)} - X_m^{(i,2)}\,\frac{2m}{\sin\theta^{(i)}}\,\frac{P_n^{-2m}(\cos\theta^{(i)})}{P_1^{-2m}(0)} \\ &\quad + \frac{n+2}{2n(2n+1)}X_m^{(i,3)}\,\frac{P_{n-1}^{-2m\prime}(\cos\theta^{(i)})}{P_1^{-2m}(0)}, \\ t_m^{(i)} &= X_m^{(i,1)}\,\frac{2m}{\sin\theta^{(i)}}\,\frac{P_{n+1}^{-2m}(\cos\theta^{(i)})}{P_1^{-2m}(0)} - X_m^{(i,2)}\,\frac{P_n^{-2m\prime}(\cos\theta^{(i)})}{P_1^{-2m}(0)} \\ &\quad + \frac{n+2}{2n(2n+1)}X_m^{(i,3)}\,\frac{2m}{\sin\theta^{(i)}}\,\frac{P_{n-1}^{-2m}(\cos\theta^{(i)})}{P_1^{-2m}(0)}. \end{aligned}\right\} \tag{3.11}$$

Here the prime denotes a derivative with respect to $\theta^{(i)}$. The sequences $q_m^{(i)}$, $s_m^{(i)}$ and $t_m^{(i)}$ depend on n but we also omit this index without loss of clarity.

The velocity field of the problem B is defined by (3.9), (3.10), (3.11) if we put $n = 1$. In the case of problem A we cannot merely set $n = 0$. A particular solution of the inhomogeneous equations (the terms containing n in the denominator) must be chosen in another form. It leads to a different representation of the functions $s_m^{(i)}$, $t_m^{(i)}$, namely

$$\left.\begin{aligned} s_m^{(i)} &= X_m^{(i,1)}\,\frac{P_1^{-2m\prime}(\cos\theta^{(i)})}{P_1^{-2m}(0)} - X_m^{(i,2)}\,\frac{2m}{\sin\theta^{(i)}}\,\frac{P_0^{-2m}(\cos\theta^{(i)})}{P_1^{-2m}(0)} \\ &\quad - X_m^{(i,3)}\,\frac{\cos\theta^{(i)}}{2m}\,\frac{P_0^{-2m\prime}(\cos\theta^{(i)})}{P_1^{-2m}(0)}, \\ t_m^{(i)} &= X_m^{(i,1)}\,\frac{2m}{\sin\theta^{(i)}}\,\frac{P_1^{-2m}(\cos\theta^{(i)})}{P_1^{-2m}(0)} - X_m^{(i,2)}\,\frac{P_0^{-2m\prime}(\cos\theta^{(i)})}{P_1^{-2m}(0)} \\ &\quad - X_m^{(i,3)}\,\cot\theta^{(i)}\,\frac{P_0^{-2m}(\cos\theta^{(i)})}{P_1^{-2m}(0)}, \end{aligned}\right\} \tag{3.12}$$

whereas the function $q_m^{(i)}$ is obtained from (3.10) by the substitution $n = 0$.

Thus, the velocity field (3.4) has nine independent sets of the Fourier coefficients $X_m^{(i,j)}$ $(i, j = 1, 2, 3)$ and, potentially, has sufficient arbitrariness for satisfaction of the nine boundary conditions (2.10).

The chosen form of the solution seems the best one for the problem under consideration. Another type of representation for the velocity field was obtained by Shankar (2000) by means of eigenfunction expansion based upon the general representation by Tran-Cong & Blake (1982). That representation, however, leads to complex eigenfunctions with unestablished asymptotic behaviour of the coefficients.

3.2. *Satisfaction of the boundary conditions*

The three spherical coordinate systems are arranged in such a way that the surface $\theta^{(i)} = \pi/2$ can also be specified by $\phi^{(j)} = 0$, or $\phi^{(k)} = \pi/2$. Here and in what follows it is assumed that the ordered triplet (i, j, k) takes the values (1, 2, 3), (2, 3, 1), (3, 1, 2). (Any subsequent triplet is obtained from a previous one via a cyclic rearrangement.) Other coordinates at the surface $\theta^{(i)} = \pi/2$ are related by $\theta^{(j)} = \phi^{(i)}$, $\theta^{(k)} = \pi/2 - \phi^{(i)}$.

From (3.4) follows that the velocity at this surface is

$$\boldsymbol{U} = r^n \left[\boldsymbol{u}^{(i)}\left(\tfrac{1}{2}\pi,\, \phi^{(i)}\right) + \boldsymbol{u}^{(j)}(\phi^{(i)},\, 0) + \boldsymbol{u}^{(k)}\left(\tfrac{1}{2}\pi - \phi^{(i)},\, \tfrac{1}{2}\pi\right)\right]. \tag{3.13}$$

The vectors $\boldsymbol{u}^{(j)}$ and $\boldsymbol{u}^{(k)}$ were originally determined in the jth and kth coordinate systems, respectively. Their components in the ith coordinate system are given by (A 4) using (A 1). At the surface $\theta^{(i)} = \pi/2$ these expressions are

$$u^{(j)}_{\theta^{(i)}} = -u^{(j)}_{\phi^{(j)}}, \quad u^{(j)}_{\phi^{(i)}} = u^{(j)}_{\theta^{(j)}}, \quad u^{(k)}_{\theta^{(i)}} = u^{(k)}_{\phi^{(k)}}, \quad u^{(k)}_{\phi^{(i)}} = -u^{(k)}_{\theta^{(k)}}. \tag{3.14}$$

Now from boundary conditions (2.10), representations (3.13), (3.9) and relations (3.14) we obtain the nine functional equations

$$\left.\begin{aligned}
&\sum_{m=1}^{\infty} q^{(i)}_m(\tfrac{1}{2}\pi)\sin 2m\phi^{(i)} = f^{(i)}(\phi^{(i)}),\\
&\sum_{m=1}^{\infty} s^{(i)}_m(\tfrac{1}{2}\pi)\sin 2m\phi^{(i)} - C^{(j)}\frac{P_n^{-1}(\cos\phi^{(i)})}{P_n^{-1}(0)} - \sum_{m=1}^{\infty} t^{(j)}_m(\phi^{(i)})\\
&\quad + C^{(k)}\frac{P_n^{-1}(\sin\phi^{(i)})}{P_n^{-1}(0)} + \sum_{m=1}^{\infty}(-1)^m t^{(k)}_m(\tfrac{1}{2}\pi - \phi^{(i)}) = 0,\\
&C^{(i)} + \sum_{m=1}^{\infty} t^{(i)}_m(\tfrac{1}{2}\pi)\cos 2m\phi^{(i)} = g^{(i)}(\phi^{(i)}).
\end{aligned}\right\} \tag{3.15}$$

The left-hand sides of the first and third triplets of equations (3.15) represent ordinary Fourier series, and, consequently,

$$q^{(i)}_m\left(\tfrac{1}{2}\pi\right) = f^{(i)}_m, \quad C^{(i)} = g^{(i)}_0, \quad t^{(i)}_m\left(\tfrac{1}{2}\pi\right) = g^{(i)}_m, \quad m = 1, 2, \ldots, \quad i = 1, 2, 3, \tag{3.16}$$

with the Fourier coefficients of the prescribed functions given as

$$\left.\begin{aligned}
f^{(i)}_m &= \frac{4}{\pi}\int_0^{\pi/2} f^{(i)}(\phi)\,\sin 2m\phi\,\mathrm{d}\phi,\\
g^{(i)}_0 = \frac{2}{\pi}\int_0^{\pi/2} g^{(i)}(\phi)\,\mathrm{d}\phi\,, &\quad g^{(i)}_m = \frac{4}{\pi}\int_0^{\pi/2} g^{(i)}(\phi)\,\cos 2m\phi\,\mathrm{d}\phi.
\end{aligned}\right\} \tag{3.17}$$

Equations (3.16) permit one to obtain the algebraic relations between the unknown coefficients and to express two sets of coefficients via the third one. For problem A these relations are

$$\frac{1}{2}\left(1 + \frac{1}{2m}\right) X^{(i,3)}_m = X^{(i,1)}_m - f^{(i)}_m, \quad \left(1 + \frac{1}{2m}\right) X^{(i,2)}_m = X^{(i,1)}_m - \frac{1}{2m} g^{(i)}_m. \tag{3.18}$$

For problem B these relations are

$$X^{(i,1)}_m = f^{(i)}_m \frac{m(2m+2)}{(2m)^2 - 1}, \quad X^{(i,3)}_m \frac{m}{2m-1} = X^{(i,2)}_m - \frac{2m}{(2m)^2 - 1}(m f^{(i)}_m - g^{(i)}_m). \tag{3.19}$$

Expansion into Fourier series of the second triplet of equations (3.15) in view of relations (3.18) and (3.19) for problems A and B, respectively, leads to a triply infinite system of linear algebraic equations.

For problem A the triply infinite system for the set of unknowns $X^{(i,1)}_m$ $(i = 1, 2, 3)$ is

$$X^{(i,1)}_m - 2m\sum_{l=1}^{\infty} D_{m,l}\left(X^{(j,1)}_l + (-1)^{m+l} X^{(k,1)}_l\right) = S^{(i)}_m, \quad m = 1, 2, \ldots \tag{3.20}$$

with the coefficients

$$D_{m,l} = \frac{4}{\pi}\int_0^{\pi/2} \cot\phi \left(\frac{1-\cos\phi}{1+\cos\phi}\right)^l \sin 2m\phi \,\mathrm{d}\phi, \quad m,\, l = 1,2,\ldots \tag{3.21}$$

For problem B the triply infinite system for the set of unknowns $X_m^{(i,2)}$ $(i = 1,2,3)$ is

$$X_m^{(i,2)} - 2m\sum_{l=1}^{\infty}\left(D_{m,l} + \frac{F_{m,l}}{2l}\right)\left(X_l^{(j,2)} + (-1)^{m+l}X_l^{(k,2)}\right) = Q_m^{(i)}, \quad m = 1,2,\ldots \tag{3.22}$$

where the coefficients are given as

$$F_{m,l} = \frac{4}{\pi}\int_0^{\pi/2} \frac{\cos^2\phi}{\sin\phi}\left(\frac{1-\cos\phi}{1+\cos\phi}\right)^l \sin 2m\phi \, d\phi, \quad m,\, l = 1,2,\ldots\ . \tag{3.23}$$

The expressions for the right-hand-side terms $S_m^{(i)}$, $Q_m^{(i)}$ are given in Appendix B. It is very difficult to express the integrals for $D_{m,l}$ and $F_{m,l}$ in closed form and in all the problems considered they were evaluated numerically.

On substitution of (3.7), (3.18) into (3.10) for $n = 0$ and (3.12), (3.9) provides the final expressions for the three vectors $\boldsymbol{u}^{(i)}$ of problem A:

$$\left.\begin{aligned}
u_r^{(i)} &= \sum_{m=1}^{\infty} f_m^{(i)} R_i^{2m} \sin 2m\phi^{(i)} + \cos\theta^{(i)} \sum_{m=1}^{\infty} X_m^{(i,1)} \frac{R_i^{2m}}{2m} \sin 2m\phi^{(i)},\\
u_{\theta^{(i)}}^{(i)} &= \frac{1}{\sin\theta^{(i)}} \sum_{m=1}^{\infty} \left(2f_m^{(i)} \cos\theta^{(i)} + g_m^{(i)}\right) R_i^{2m} \sin 2m\phi^{(i)}\\
&\quad - \sum_{m=1}^{\infty} X_m^{(i,1)} \left(\cot\theta^{(i)} + \frac{1}{2m}\sin\theta^{(i)}\right) R_i^{2m} \sin 2m\phi^{(i)},\\
u_{\phi^{(i)}}^{(i)} &= g_0^{(i)} R_i + \frac{1}{\sin\theta^{(i)}} \sum_{m=1}^{\infty} \left(2f_m^{(i)} \cos\theta^{(i)} + g_m^{(i)}\right) R_i^{2m} \cos 2m\phi^{(i)}\\
&\quad - \cot\theta^{(i)} \sum_{m=1}^{\infty} X_m^{(i,1)} R_i^{2m} \cos 2m\phi^{(i)},
\end{aligned}\right\} \tag{3.24}$$

where the following notation was introduced:

$$R_i = \left(\frac{1-\cos\theta^{(i)}}{1+\cos\theta^{(i)}}\right)^{1/2} = \tan\frac{\theta^{(i)}}{2}.$$

The final expressions for $\boldsymbol{u}^{(i)}$ in problem B can be obtained by substitution (3.7), (3.8), (3.19) into (3.9), (3.10), (3.11) for $n = 1$.

3.3. *Asymptotic analysis of the solution*

A traditional method of solution of infinite systems is the method of simple reduction (see Kantorovich & Krylov 1964 for further details) based upon truncation of an infinite system to a finite one, solving it by any available technique and subsequent increase of the number of unknowns and equations involved. However, one needs first to analyse the asymptotic behaviour of the unknowns. If they do not decrease or decrease slowly, the truncation of the system may cause unacceptable errors. The asymptotic analysis of the systems in question was performed by means of the Mellin transform technique similar to Gomilko (1993) and Meleshko & Gomilko (1997). In

our case the Mellin transformation could not be directly applied to the algebraic system (3.20). The first step consisted in reducing the triply infinite algebraic system to a system of three integral equations.

The final result for the unknowns of system (3.20) is

$$X_m^{(i,1)} = A^{(i)} + x_m^{(i)}, \quad m = 1, 2, \ldots, \tag{3.25}$$

where the leading terms and the order of the remainders are

$$\left.\begin{aligned} A^{(1)} &= -\frac{8}{\pi^2 - 4}\left[g^{(1)}(0) + (-1)^m g^{(1)}(\tfrac{1}{2}\pi)\right], \quad A^{(2)} = \frac{4\pi}{\pi^2 - 4} g^{(1)}(\tfrac{1}{2}\pi), \\ A^{(3)} &= (-1)^m \frac{4\pi}{\pi^2 - 4} g^{(1)}(0), \quad x_m^{(i)} = O\left(\frac{\ln m}{m}\right), \quad m \to \infty. \end{aligned}\right\} \tag{3.26}$$

Such a logarithmic behaviour was also reported by Meleshko, Malyuga & Gomilko (2000) for the lidded cylindrical cavity problem. Notice that if $g^{(1)}(0) \neq 0$ or $g^{(1)}(\pi/2) \neq 0$ then the unknowns $X_m^{(i,1)}$ do not tend to zero with $m \to \infty$. This causes a problem for the direct application of the simple reduction method.

Knowledge of the asymptotic behaviour of the unknowns provides a way of using the method of simple reduction. Relations (3.25) permit one to introduce the new unknowns $x_m^{(i)}$ that tend to zero as m tends to infinity. Substitution of these relations into (3.20) provides an infinite system for the new unknowns which can be successfully truncated.

The asymptotic behaviour of the unknowns (3.25) with (3.26) also provides a way of considerably improving convergence of the series included in the solution. This procedure is necessary for the accurate evaluation of the velocity near the boundary of the corner, where the series converge slowly, and thus truncation of them may cause impermissible numerical errors. It consists in substitution of (3.25) into the three vector fields (3.24) and replacement of the series inclusive of $A^{(i)}$ by their sums (Prudnikov, Brychkov & Marichev 1986). The series containing the new unknowns $x_m^{(i)}$ converge more rapidly.

Taking into account the asymptotic behaviour of the sums, along with the asymptotic behaviour of the series including $f_m^{(i)}$, $g_m^{(i)}$, one can derive the local velocity near the edge $\theta^{(2)} = 0$. The mathematical manipulations are not complicated but are rather cumbersome. The final result is presented in the system $(r, \theta^{(2)}, \phi^{(2)})$ as follows:

$$\left.\begin{aligned} u_r^{loc} &= f^{(1)}(0)\left(1 - \frac{2\phi^{(2)}}{\pi}\right), \\ u_{\theta^{(2)}}^{loc} &= g^{(1)}(0)\left\{\cos\phi^{(2)} - \frac{4}{\pi^2 - 4}\left[\tfrac{1}{2}\pi\phi^{(2)}\cos\phi^{(2)} + (\tfrac{1}{2}\pi - \phi^{(2)})\sin\phi^{(2)}\right]\right\}, \\ u_{\phi^{(2)}}^{loc} &= g^{(1)}(0)\frac{4}{\pi^2 - 4}\left[\phi^{(2)}\cos\phi^{(2)} - \tfrac{1}{2}\pi(\tfrac{1}{2}\pi - \phi^{(2)})\sin\phi^{(2)}\right]. \end{aligned}\right\} \tag{3.27}$$

The components $u_{\theta^{(2)}}^{loc}$, $u_{\phi^{(2)}}^{loc}$ coincide with the radial and angular components, respectively, of the velocity field in the two-dimensional corner with angle $\pi/2$ found by Goodier (1934) and Taylor (1962); see also Batchelor (1967, p. 224).

Numerical tests of satisfaction of the boundary conditions by the normal velocity components $u_{\theta^{(1)}}$ at the wall $\theta^{(1)} = \pi/2$ and $u_{\phi^{(1)}}$ at $\phi^{(1)} = 0$ and $\phi^{(1)} = \pi/2$ show an accuracy of within 0.1% near the edges and much less inside the walls. The tangential velocity components satisfy the boundary conditions identically. It is worth noting

that this accuracy can even be increased by taking into account not only the first but also the higher-order terms of the asymptotic expansion of the unknowns.

It should be mentioned that, in contrast to the particular problem considered in Hills & Moffatt (2000), where, due to the specific geometry of a dihedral corner and the stated boundary conditions, the singular terms of stress are cancelled in the expression for the total force on the blade, in the case under consideration, these terms integrate to produce an infinite total force on the fixed walls.

4. Streamline structure

The families of streamlines of both problems A and B are given by the system of differential equations

$$\frac{\mathrm{d}r}{u_r} = \frac{r\,\mathrm{d}\theta^{(i)}}{u_{\theta^{(i)}}} = \frac{r\,\sin\theta^{(i)}\,\mathrm{d}\phi^{(i)}}{u_{\phi^{(i)}}}. \tag{4.1}$$

Separation of the radial and geographical coordinates followed by integration along a streamline provides the first integral of motion. It expresses the radial coordinate of an individual particle in terms of its geographical coordinates and the initial position

$$\frac{r}{r_0} = \exp\left(\int_{\theta_0^{(i)}}^{\theta^{(i)}} \frac{u_r\,\mathrm{d}\theta^{(i)}}{u_{\theta^{(i)}}}\right) = \exp\left(\int_{\phi_0^{(i)}}^{\phi^{(i)}} \frac{u_r\,\sin\theta^{(i)}\,\mathrm{d}\phi^{(i)}}{u_{\phi^{(i)}}}\right), \tag{4.2}$$

where the integrals are taken along the projection of the streamline on a spherical surface, and $(r_0, \theta_0^{(i)}, \phi_0^{(i)})$ is the initial position of the particle. Taking into account the continuity equation, one can present (4.2) as follows

$$\frac{r}{r_0} = \exp\left(-\frac{1}{n+2}\int_{(\theta_0^{(i)},\phi_0^{(i)})}^{(\theta^{(i)},\phi^{(i)})} \frac{\nabla\cdot\boldsymbol{u}_s}{u_s}\,\mathrm{d}l\right). \tag{4.3}$$

Here $\boldsymbol{u}_s = (0, u_{\theta^{(i)}}, u_{\phi^{(i)}})$. In problem A, $\boldsymbol{u}_s$ represents the velocity of the particle motion over the sphere of radius r. The element $\mathrm{d}l$ is an elementary arc on this sphere. From (4.3) we arrive at the following conclusion valid for problem A: if any elementary material volume moves away from the vertex, the area of its cross-section through the sphere of radius r decreases. A motion towards the vertex increases the area of the cross-section by the sphere. In problem B, $\boldsymbol{u}_s$ is the velocity of the particle projection on the unit sphere. The integral (4.3) also leads to another conclusion. If an elementary volume moves away from the vertex, the area of its projection on the unit sphere decreases. A motion towards the vertex increases the area of the projection on the unit sphere.

The numerical analysis of several flows driven by the motion of a rigid lid is performed on the basis of the solutions derived in § 3. The flow induced by a uniform translation of the bottom wall is a simple, practically realizable example of problem A. The motion of the wall parallel to its bisectrix generates a symmetric velocity field. For definiteness, let the wall move toward the vertex, i.e. in the direction of the angle $\gamma = 5\pi/4$ to the positive direction of the X-axis. If the direction of the wall translation is perpendicular to the bisectrix (say, $\gamma = 3\pi/4$), the induced flow is an example of the antisymmetric problem.

Streamline patterns of the symmetric and antisymmetric flows of problem A are presented in figures 2(a) and 2(b), respectively. The streamlines of the symmetric flow are non-closed. The motion in the plane of symmetry $\phi^{(1)} = \pi/4$ is strictly two-dimensional. In the antisymmetric velocity field the streamlines are closed. This

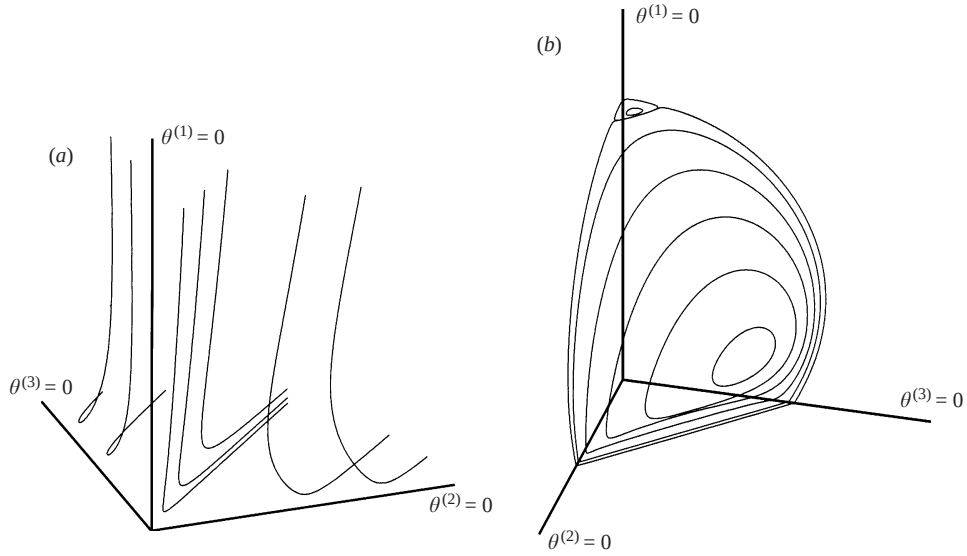

FIGURE 2. Streamline patterns for problem A. (*a*) The bottom wall moves along its bisectrix. (*b*) The bottom wall moves in a direction perpendicular to its bisectrix.

follows from the symmetry of the streamlines about the plane $\phi^{(1)} = \pi/4$. If any of them intersects that plane twice, it is closed.

The primary eddy that occupies the region adjacent to the bottom wall is separated from the secondary eddy situated in the neighbourhood of the stationary edge $\theta^{(1)} = 0$ by a dividing surface. The intersection of that surface and a sphere is a line, referred to as a separatrix. The point of intersection of the separatrix and the sidewall $\phi^{(1)} = 0$ is determined by the condition of zero shear stress. Let its position be $(r, \theta^*, 0)$. The angle of inclination of the separatrix to the sidewall can be evaluated in the local spherical coordinate system $(r, \theta^{(loc)}, \phi^{(loc)})$ with the origin at the vertex. The axis $\theta^{(loc)} = 0$ coincides with the line $\theta^{(1)} = \theta^*$, $\phi^{(1)} = 0$. The system $(r, \theta^{(1)}, \phi^{(1)})$ can be readily transformed to the system $(r, \theta^{(loc)}, \phi^{(loc)})$ by a rotation through the angle θ^* about the axis $\theta^{(1)} = \pi/2$, $\phi^{(1)} = \pi/2$. The next step is based on the Taylor expansion of the velocity field near $\theta^{(loc)} = 0$. It leads to the following equations for the determination of the position of the point and the angle of inclination of the separatrix:

$$\left.\frac{\partial u_{\theta^{(1)}}}{\partial \phi^{(1)}}\right|_{(r,\theta^*,0)} = 0, \quad \tan\phi^{(loc)} = -\left(2\sin\theta^* \frac{\partial^2 u_{\theta^{(1)}}}{\partial\theta^{(1)}\partial\phi^{(1)}} - \frac{\partial^2 u_{\phi^{(1)}}}{\partial\phi^{(1)2}}\right) \Bigg/ \frac{\partial^2 u_{\theta^{(1)}}}{\partial\phi^{(1)2}}$$

$$\text{at} \quad \theta^{(1)} = \theta^*, \quad \phi^{(1)} = 0. \tag{4.4}$$

In view of the linearity of the problem, the velocity of the flow driven by the translation of the bottom wall in the direction of some angle γ can be presented as a linear combination of the corresponding symmetric and antisymmetric fields:

$$\boldsymbol{U} = -\cos\left(\gamma - \frac{\pi}{4}\right) \boldsymbol{U}_s + \sin\left(\gamma - \frac{\pi}{4}\right) \boldsymbol{U}_a, \tag{4.5}$$

where $\boldsymbol{U}_s$ and $\boldsymbol{U}_a$ are symmetric and antisymmetric velocity fields, respectively. Figure 3(*a*) shows the streamline plot for $\cot(\gamma - \pi/4) = -0.1$. One can observe the appearance of spirals as a result of the combination of the rotation generated by the antisymmetric part and the motion caused by the symmetric part. When increasing

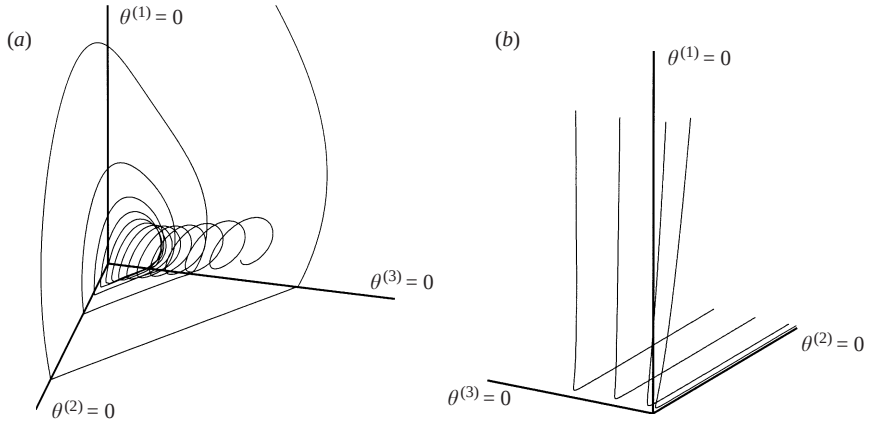

FIGURE 3. Streamline patterns for problem A. (*a*) $\cot(\gamma - \pi/4) = -0.1$; (*b*) $\cot(\gamma - \pi/4) = -1$, the wall moves parallel to the edge $\theta^{(2)} = 0$.

the absolute value of $\cot(\gamma - \pi/4)$, the spirals become less tightly wound. They are not seen in figure 3(*b*), which illustrates the streamline patterns for $\cot(\gamma - \pi/4) = -1$. In this case the bottom wall moves parallel to the edge. Near the stationary edge, the spirals are not observed even for small $|\cot(\gamma - \pi/4)|$. This result is not unexpected as the Poiseuille flow in a dihedral corner has velocity of order $\rho^2 \log \rho$ (Moffatt & Duffy 1980), where ρ is distance from the edge. It dominates over Moffatt's velocity field, which is of the order about $\rho^{2.74}$ (Moffatt 1964).

The flow induced by the uniform rotation of the bottom wall about the vertex is a simple, experimentally realizable example of problem B. The local behaviour of the flow near the stationary edge $\theta^{(1)} = 0$ was analysed by Hills & Moffatt (2000), who considered the trihedral corner as a limiting case of a cone partitioned by two rigid triangular fins. The power dependence of the dominant term of the velocity on $\theta^{(1)}$ (in our notation) with a complex exponent led the authors to the conclusion that a sequence of eddies existed near the stationary edge. The streamlines shown in figure 4 lie on a sphere with its centre at the vertex. As a consequence of the velocity field symmetries, the streamlines are closed and symmetric about the plane $\phi^{(1)} = \pi/4$. The secondary eddy near the stationary edge confirms the asymptotic analysis by Hills & Moffatt (2000).

Now let us turn to problem C. Let the wall rotate with the angular velocity Ω about the point $M(x_0, y_0)$. As already pointed in § 2, a solution of problem C can be found as a sum of solutions of problems A and B if we put $U_0 \sin\gamma = -\Omega x_0$, $U_0 \cos\gamma = \Omega y_0$. From (4.5) follows that the dimensionless velocity is represented as a superposition of the three above-described velocities:

$$\frac{\boldsymbol{U}}{U_0} = \frac{1}{\sqrt{2}\,U_0}\left[\frac{x_0 - y_0}{R}\boldsymbol{U}_s - \frac{x_0 + y_0}{R}\boldsymbol{U}_a\right] + \frac{r}{R}\boldsymbol{u}_\Omega, \tag{4.6}$$

where $(r/R)\,\boldsymbol{u}_\Omega$ is the dimensionless velocity of the flow induced by the wall rotation about the vertex, and $R = (x_0^2 + y_0^2)^{1/2}$ is distance OM. Integral (4.3) is not valid for such flows. The flow behaviour may change significantly with the ratio r/R. Two simple examples illustrate the three-dimensional nature of the streamlines.

If the centre M is on the bisectrix ($x_0 = y_0$), representation (4.6) is simplified to a combination of only two antisymmetric velocities. It is essential that the centre of the wall rotation is inside the corner, as in this case the two terms are opposite

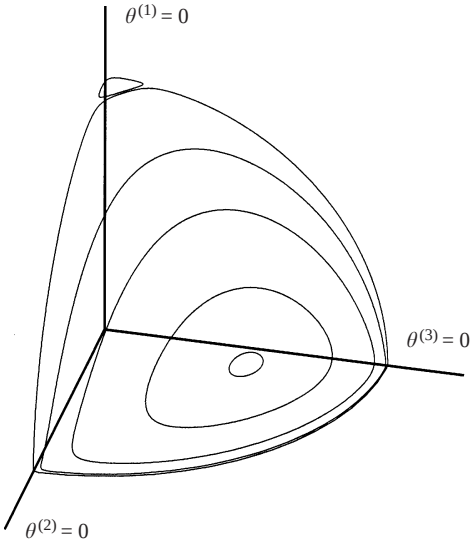

FIGURE 4. Streamline patterns for problem B. The flow is induced by the rotation of the bottom wall about the vertex.

in sign. The first of them dominates near the vertex $r \ll R$, whereas the second term contributes to the velocity at some distance from the vertex. Figure 5(a) shows the streamline patterns of the flow. The behaviour of the streamlines of the eddy structures close to the stationary edge is of particular interest. The stagnation lines (lines of zero velocity) are presented in figure 5(b). They lie in the plane $\phi^{(1)} = \pi/4$. The three-dimensionality of the problem results in the different nature of the flow near different points of the common stagnation line. As one can see from figure 5(c), where the streamlines near the vertex are shown, the stagnation line consists of centres at small and large distances from the vertex. These parts of the curve are connected via a segment composed of saddles. Such a behaviour, which has not been observed in the quasi-two-dimensional flows discussed above, shows that the three-dimensional corner structures are more complicated and may have not only the nature of an eddy.

If point M is on the straight line passing through the vertex and perpendicular to the bisectrix of the bottom side of the corner ($x_0 = -y_0$), the second term in representation (4.6) vanishes. Streamlines for this flow are presented in figure 5(d). The combination of the symmetric and antisymmetric fields leads to the appearance of spirally shaped streamlines.

The difference in behaviour of a streamline near to and far away from the vertex is especially noticeable when M is close to the bisectrix of the bottom wall. Figure 6(a) shows a streamline in the case that $(x_0 - y_0)/(x_0 + y_0) = \cot(\gamma - \pi/4) = -0.1$. Now all three terms in (4.6) are non-zero. An enlarged view of the portion of the curve situated in the vicinity of the vertex is shown in figure 6(b). Because of the insignificant role of the term $r/R\,\boldsymbol{u}_\Omega$ at small r/R, the streamline bears some resemblance to the curve shown in figure 3(a).

5. Conclusions

The essential results of the paper are the following. The method of superposition was successfully applied to solve the Stokes problem in the trihedral corner with a

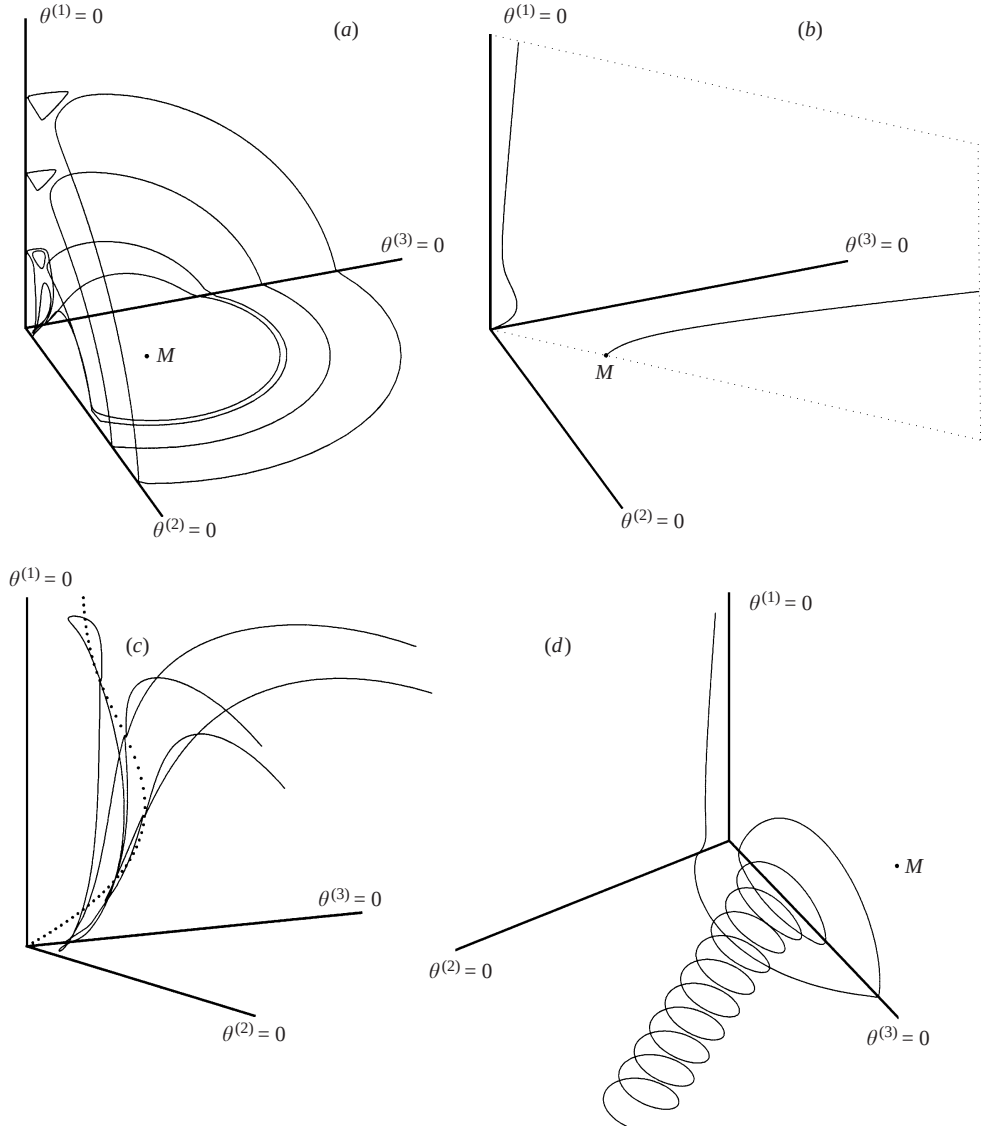

FIGURE 5. Problem C. The bottom wall rotates about the centre M displaced from the vertex of the corner. In (*a–c*) the centre M is on the bisectrix of the wall. (*a*) Streamline patterns; (*b*) stagnation lines; (*c*) streamlines in the neighbourhood of the vertex; the stagnation line (dotted line) includes both centres and saddles. (*d*) The winding streamline; the centre M is on the perpendicular to the bisectrix, which passes through the vertex.

non-zero tangential velocity prescribed at one wall. The analysis of the asymptotic behaviour of the unknown coefficients provided a way of refining the technique to obtain high accuracy everywhere in the corner. The velocity field was shown to behave near the edges, where the discontinuity of the tangential velocities was preassigned, in accordance with the Goodier–Taylor solution in a two-dimensional corner of angle $\pi/2$. The numerical analysis of the flow topology near the edge formed by two fixed walls confirmed the existence of eddies.

The flow driven by the wall rotation about the vertex was shown to be strictly

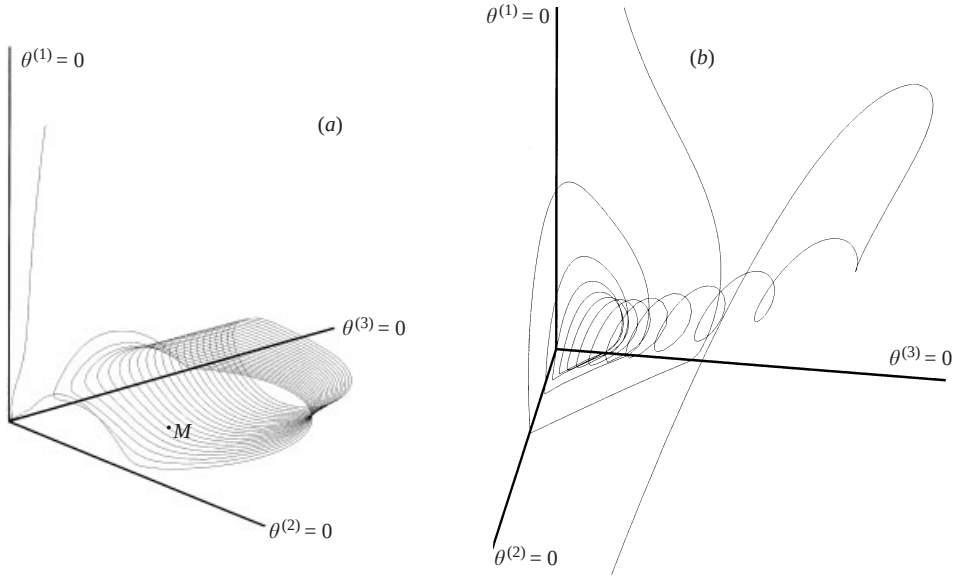

FIGURE 6. Problem C. One streamline of the flow induced by the rotation of the bottom wall about M at $(x_0 - y_0)/(x_0 + y_0) = \cot(\gamma - \pi/4) = -0.1$. (*a*) The general view. (*b*) An enlarged view of the region close to the vertex.

two-dimensional. In this special case the streamlines are closed and lie on a spherical surface. An integral of the motion was found in the case that the velocity was of the form $\boldsymbol{U} = r^n \boldsymbol{u}$, where $\boldsymbol{u}$ was a function of only the physical coordinates. Such flows are quasi-two-dimensional. Although all three scalar components of the velocity may be non-zero, only the physical coordinates of an individual particle are independent. As an example the flow driven by the wall translation in a tangential direction was studied.

The flow becomes essentially three-dimensional if the wall rotates about a centre displaced from the vertex. Integral (4.3) is not valid for such flows. The corner structures near the stationary edge are more complicated. The stagnation lines, usually considered as centrelines of the corner eddies, may contain saddle points.

A similar method is used for the cases where the planes are not orthogonal. In such cases the results may be qualitatively similar to those given here if the angles between the planes are near $\pi/2$, but otherwise could be rather different. This problem still remains challenging.

We are grateful to Professor V. T. Grinchenko from the Institute of Hydromechanics, Kiev and Professor A. F. Ulitko from Kiev University for helpful discussions concerning the vector structure of the three-dimensional Stokes problem. Our thanks also go to referees for suggestions that led to improvement in presentation of the paper.

Appendix A

Three spherical coordinate systems $(r, \theta^{(i)}, \phi^{(i)})$, $i = 1, 2, 3$, shown in figure 1 are introduced in such a way that the axis $\theta^{(i)} = 0$ coincides with the axes $\theta^{(j)} = \pi/2$, $\phi^{(j)} = \pi/2$ and $\theta^{(k)} = \pi/2$, $\phi^{(k)} = 0$. The triplet (i, j, k) takes the values (1, 2, 3), (2, 3, 1), (3, 1, 2). The second and third values are obtained from the first one

by cyclic rearrangements. The simplest way of deriving a relationship between the coordinate systems is the following. First, the spherical coordinates $(r, \theta^{(i)}, \phi^{(i)})$ are transformed into the corresponding Cartesian coordinates $(x_1^{(i)}, x_2^{(i)}, x_3^{(i)})$. It is easy to see that $(x_1^{(i)}, x_2^{(i)}, x_3^{(i)}) = (x_3^{(j)}, x_1^{(j)}, x_2^{(j)}) = (x_2^{(k)}, x_3^{(k)}, x_1^{(k)})$. Then returning to the spherical coordinates we obtain the relations

$$\left.\begin{aligned} \cos\theta^{(j)} &= \sin\theta^{(i)}\cos\phi^{(i)}, \quad \cot\phi^{(j)} = \tan\theta^{(i)}\sin\phi^{(i)}, \\ \cos\theta^{(k)} &= \sin\theta^{(i)}\sin\phi^{(i)}, \quad \cot\phi^{(k)} = \cot\theta^{(i)}\sec\phi^{(i)}. \end{aligned}\right\} \tag{A 1}$$

Relations between the components of a vector field $\boldsymbol{U}$ in three spherical coordinate systems with a common origin can be derived as follows.

The unit coordinate vectors of the spherical coordinate system $(r, \theta^{(i)}, \phi^{(i)})$, $i = 1, 2, 3$, are related by

$$\boldsymbol{e}_{\theta^{(i)}} = \frac{\partial \boldsymbol{e}_r}{\partial\theta^{(i)}}, \quad \boldsymbol{e}_{\phi^{(i)}} = \frac{1}{\sin\theta^{(i)}}\frac{\partial \boldsymbol{e}_r}{\partial\phi^{(i)}}. \tag{A 2}$$

These equations may be readily obtained from the definition of unit coordinate vectors as derivatives of a radius-vector with respect to arcs of the corresponding coordinate curves. Considering $\theta^{(i)}$, $\phi^{(i)}$ as functions of $\theta^{(s)}$, $\phi^{(s)}$, $s = 1, 2, 3$ we can rewrite (A 2) as

$$\boldsymbol{e}_{\theta^{(i)}} = \frac{\partial \boldsymbol{e}_r}{\partial\theta^{(s)}}\frac{\partial\theta^{(s)}}{\partial\theta^{(i)}} + \frac{\partial \boldsymbol{e}_r}{\partial\phi^{(s)}}\frac{\partial\phi^{(s)}}{\partial\theta^{(i)}}, \quad \boldsymbol{e}_{\phi^{(i)}} = \frac{1}{\sin\theta^{(i)}}\left(\frac{\partial \boldsymbol{e}_r}{\partial\theta^{(s)}}\frac{\partial\theta^{(s)}}{\partial\phi^{(i)}} + \frac{\partial \boldsymbol{e}_r}{\partial\phi^{(s)}}\frac{\partial\phi^{(s)}}{\partial\phi^{(i)}}\right). \tag{A 3}$$

Equations (A 2) have the same form in the sth coordinate system. Substituting them into (A 3) and then multiplying the left- and right-hand sides by the vector $\boldsymbol{U}$, we obtain the relations

$$\left.\begin{aligned} U_{\theta^{(i)}} &= U_{\theta^{(s)}}\frac{\partial\theta^{(s)}}{\partial\theta^{(i)}} + U_{\phi^{(s)}}\sin\theta^{(s)}\frac{\partial\phi^{(s)}}{\partial\theta^{(i)}}, \\ U_{\phi^{(i)}} &= \frac{1}{\sin\theta^{(i)}}\left(U_{\theta^{(s)}}\frac{\partial\theta^{(s)}}{\partial\phi^{(i)}} + U_{\phi^{(s)}}\sin\theta^{(s)}\frac{\partial\phi^{(s)}}{\partial\phi^{(i)}}\right). \end{aligned}\right\} \tag{A 4}$$

Equations (A 4) relate components of the velocity vector $\boldsymbol{U}$ in two arbitrary spherical coordinate systems with a common origin.

Appendix B

The right-hand-side terms in the infinite system (3.20) are

$$\begin{aligned} S_m^{(i)} = {} & -4m\chi_m\left(g_0^{(j)} + (-1)^m g_0^{(k)}\right) + 2mg_m^{(i)} \\ & -4m\sum_{l=1}^{\infty} D_{m,l}\left(f_l^{(j)} + (-1)^{m+l} f_l^{(k)}\right) - 2m\sum_{l=1}^{\infty} E_{m,l}\left(g_l^{(j)} + (-1)^{m+l} g_l^{(k)}\right), \end{aligned} \tag{B 1}$$

where

$$\left.\begin{aligned} \chi_m &= \frac{2}{\pi}\int_0^{\pi/2}\left(\frac{1-\cos\phi}{1+\cos\phi}\right)^{1/2}\sin 2m\phi\,\mathrm{d}\phi, \\ E_{m,l} &= \frac{4}{\pi}\int_0^{\pi/2}\frac{1}{\sin\phi}\left(\frac{1-\cos\phi}{1+\cos\phi}\right)^{l}\sin 2m\phi\,\mathrm{d}\phi, \quad m, l = 1, 2, \ldots. \end{aligned}\right\} \tag{B 2}$$

The right-hand-side terms in the infinite system (3.22) are

$$Q_m^{(i)} = \frac{4}{\pi}\frac{(2m)^2}{(2m)^2-1}\left((-1)^m g_0^{(j)} + g_0^{(k)}\right) + 2m\left(g_m^{(i)} - \frac{3m}{(2m)^2-1} f_m^{(i)}\right)$$

$$-3m\sum_{l=1}^{\infty}\frac{2l}{(2l)^2-1}(2lD_{m,l} + F_{m,l})\left(f_l^{(j)} + (-1)^{m+l} f_l^{(k)}\right)$$

$$-2m\sum_{l=1}^{\infty} E_{m,l}\left(g_l^{(j)} + (-1)^{m+l} g_l^{(k)}\right). \tag{B 3}$$

REFERENCES

Abramowitz, M. & Stegun, I. A. 1965 *Handbook of Mathematical Functions*. Dover.

Batchelor, G. K. 1967 *An Introduction to Fluid Dynamics*. Cambridge University Press.

Dean, W. R. & Montagnon, P. E. 1949 On the steady motion of viscous liquid in a corner. *Proc. Camb. Phil. Soc.* **45**, 389–395.

Gomilko, A. M. 1993 On one class of infinite systems of linear algebraic equations. *Comput. Maths Math. Phys.* **33**, 865–877.

Goodier, J. N. 1934 An analogy between the slow motion of a viscous fluid in two dimensions, and systems of plane stress. *Phil. Mag.* (7) **17**, 554–576.

Happel, J. & Brenner, H. 1965 *Low Reynolds Number Hydrodynamics*. Prentice-Hall.

Hills, C. P. & Moffatt, H. K. 2000 Rotary honing: a variant of the Taylor paint-scraper problem. *J. Fluid Mech.* **418**, 119–135.

Kantorovich, L. V. & Krylov, V. I. 1964 *Approximate Methods of Higher Analysis*. Wiley.

Lamb, H. 1932 *Hydrodynamics*, 6th edn. Cambridge University Press.

Meleshko, V. V. & Gomilko, A. M. 1997 Infinite systems for a biharmonic problem in a rectangle. *Proc. R. Soc. Lond.* A **453**, 2139–2160.

Meleshko, V. V., Malyuga, V. S. & Gomilko, A. M. 2000 Steady Stokes flow in a finite cylinder. *Proc. R. Soc. Lond.* A **456**, 1741–1758.

Moffatt, H. K. 1964 Viscous and resistive eddies near a sharp corner. *J. Fluid Mech.* **18**, 1–18.

Moffatt, H. K. & Duffy, B. R. 1980 Local similarity solutions and their limitations. *J. Fluid Mech.* **96**, 299–313.

Prudnikov, A. P., Brychkov, Yu. A. & Marichev, O. I. 1986 *Integrals and Series. Vol. 1: Elementary Functions*. Gordon & Breach.

Shankar, P. N. 2000 On Stokes flow in a semi-infinite wedge. *J. Fluid Mech.* **422**, 69–90.

Shankar, P. N. & Deshpande, M. D. 2000 Fluid mechanics in the driven cavity. *Annu. Rev. Fluid Mech.* **32**, 93–136.

Taylor, G. I. 1962 On scraping viscous fluid from a plane surface. In *Miszellangen der Angewandten Mechanik* (ed. M. Schäfer), pp. 313–315. Akademie.

Tran-Cong, T. & Blake, J. R. 1982 General solutions of the Stokes' flow equations. *J. Math. Anal. Appl.* **90**, 72–84.